Thermochimica Acta, 224 (1993) 247–259
Elsevier Science Publishers B.V., Amsterdam

Photocatalysed synthesis, characterisation and thermal behaviour of molybdenum(IV) and tungsten(IV) complexes with oxine

S.I. Ali * and N.K.S. Pundhir

Department of Chemistry, Jamia Millia Islamia, New Delhi (India)

(Received 19 October 1992; accepted 8 January 1993)

Abstract

The synthesis of adducts and complexes of molybdenum and tungsten with 8-hydroxyquinoline (oxine) starting from octacyanomolybdate(IV) and octacyanotungstate(IV) on exposure to UV irradiation in the ligand field bands was carried out. The intermediate red products, the heptacyano complexes of molybdenum(V) and tungsten(V), obtained by primary photochemical reaction, form adducts with 8-hydroxyquinoline as shown by the strong peak in the range 2200–2000 cm^{-1} due to $-C{\equiv}N$ stretching and by another peak in the range 1150–1100 cm^{-1} for the ν(C–O) stretching mode of 8-hydroxyquinoline. The final blue photolysis product reacts with oxine, with the removal of the remaining cyano groups and formation of the final complex with the latter. The thermal behaviour of these adducts and complexes were studied.

INTRODUCTION

Ultraviolet irradiation in the ligand field bands of the octacyano complexes of molybdenum(IV) and tungsten(IV) in an alkaline medium first results in the substitution of one cyanide ligand by water [1]. This primary photochemical reaction is followed by secondary thermal steps, resulting in the loss of further three-cyanide ligands and the formation of a complex of the type $[M(CN)_4O(OH)]^{3-}$ [2, 3].

A photocatalytic system based on the photochemical generation of cyanide from octacyanomolybdate(IV) and octacyanotungstate(IV) was developed by Hennig et al. [4, 5]. The formation of tetracyano bis(phenanthroline) molybdenum(IV) [6] is possible by the irradiation of octacyanomolybdate(IV) in methanol/water mixture in the presence of 1,10-phenanthroline (phen). The cyanide ligands are completely substituted in the photocatalytic system with the formation of $[W(OCH_3)_4phen]$,

---

* Corresponding author.

$[W(OC_2H_5)_4phen]$ and other similar compounds [7]. The reaction mechanism of $W(CN)_8^{4-}$ with 1,10-phenanthroline (phen) and ethanolamine (en) in a photocatalysed system has already been formulated [8, 9].

In continuation to our earlier work [10, 11], the adducts and complexes of $Mo(CN)_8^{4-}$ and $W(CN)_8^{4-}$ with oxine were synthesised in a photocatalytic system. The adducts and complexes were characterised using elemental analysis and Fourier transform (FT) infrared spectroscopy. The thermal behaviour of these compounds was also studied from their TG and DTG thermograms.

MATERIALS AND METHODS

The potassium cyanide, potassium molybdate, potassium tungstate, potassium borohydride, 8-hydroxyquinoline and the other chemicals used were of AnalaR grade. Potassium octacyanomolybdate(IV) dihydrate $K_4Mo(CN)_8 \cdot 2H_2O$ and potassium octacyanotungstate dihydrate $K_4W(CN)_8 \cdot 2H_2O$ were prepared [12] and purified in a water–ethanol mixture. The products were dried over fused $CaCl_2$. A 0.1 M 8-hydroxyquinoline (oxine) solution was prepared in 0.1 N acetic acid which was neutralised by ammonia and then reacidified with a few drops of acetic acid [13].

PREPARATION OF THE COMPLEXES

Heptacyano(8-hydroxyquinoline) molybdenum(IV)

A 0.1 M aqueous solution of potassium octacyanomolybdate(IV) (50 ml) was irradiated by ultraviolet radiation at ≈365 nm. The octacyanomolybdate, $[Mo(CN)_8)]^{4-}$, undergoes photolysis resulting in the formation of an intermediate red product, the heptacyano complex, $[Mo(CN)_7(H_2O)]^{3-}$. A 0.1 M oxine solution in acetic acid was added dropwise into the heptacyano complex with formation of the yellow adduct; this was digested on a water bath for 1 h, then filtered off and washed with an ethanol–water mixture. The adduct was dried in vacuum over fused $CaCl_2$. The adduct was analysed for $[K_3Mo(CN)_7] \cdot (C_9H_7ON)_7 \cdot 5H_2O$ (**I**).

Dicyanodioxotetraoxinato tungsten(IV)

The synthesis of the red hydrolysis product of potassium octacyanotungsten(IV) was obtained by ultraviolet irradiation of an aqueous solution of $[W(CN)_8)]^{4-}$. Oxine solution was added dropwise forming a greenish precipitate. The precipitate was kept overnight, filtered off, washed with ethanol–water mixture and dried over fused calcium chloride. The complex thus obtained was analysed for $K_2WO_2(CN)_2 \cdot (C_9H_7ON)_4 \cdot 0.5H_2O$ (**II**).

Dioxodioxinato molybdenum(IV)

A 0.1 M potassium octacyanomolybdate(IV) solution (50 ml) was irradiated with ultraviolet light of wavelength ≈365 nm for approximately 24 h until the final blue product $[Mo(CN)_4O(OH)]^{3-}$ was obtained. Oxine solution was added slowly, resulting in the formation of a reddish precipitate which was kept overnight for ageing and washed with ethanol–water mixture. The complex was dried in vacuum on fused calcium chloride and then analysed for $MoO_2(C_9H_6ON)_2$ (**III**).

Dioxodioxinato tungsten(IV)

Potassium oxy-hydroxocyanotungstate(IV) was obtained as the final blue product by the photolysis of octacyanotungstate(IV), $[W(CN)_8]^{4-}$, on irradiating it with ultraviolet light of wavelength ≈365 nm for 24 h. The blue cyanide was diluted with water and oxine solution was added to it to form the precipitate, which was kept overnight, and filtered off after digestion for an hour on a water bath. The product was dried in vacuum over fused calcium chloride and analysed for $WO_2(C_9H_6ON)_2$ (**IV**).

PHYSICAL MEASUREMENTS

Fourier transform infrared spectra were recorded in KBr matrix with a Bio-Red Digilab FTS-40. A Fourier transform Michelson interferometer equipped with highly sensitive Hg-CdTe detectors and a KBr beam splitter was used in the wavelength range 400–450 cm^{-1}. The thermal studies were carried out on a Du Pont 1090 thermal analyser with a TGA module 951. The insolubility of the complex compounds in common organic solvents prevented conductance measurements from being made.

RESULTS AND DISCUSSION

The elemental analyses of the adduct complexes are given in Table 1, together with their physical properties. The chemical composition of the adduct complexes shows that the addition of oxine to the intermediate and final photolysis products of $[Mo(CN)_8)]^{4-}$ and $[W(CN)_8)]^{4-}$ occurs in different ways. Oxine forms the adduct compounds heptacyanoheptaoxinato molybdenum(IV) and complex dicyanodioxotetraoxinate tungsten(IV), with the intermediate photolysis products being octacyanomolybdate(IV) and octacyanotungstate(IV), while with the final blue photochemical product $K_3[MO(OH)(CN)_4]$, the four cyanide groups are replaced by oxine groups to form a complex of the type $MO_2(C_9H_6ON)_2$ (where M = Mo or W).

FTIR spectra of compounds **I** and **II** (Fig. 1) exhibit strong bands in the

TABLE 1

Physical characteristics and elemental analyses of the complexes

	Elemental analysis in % [a]			
Colour	C	H	N	M is Mo or W
$K_3[Mo(CN)_7] \cdot (C_9H_7ON)_7 \cdot 5H_2O$				
Yellow	55.21	4.04	14.28	6.23
	(56.38)	(4.43)	(13.15)	(6.44)
$K_2[WO_2(CN)_2] \cdot (C_9H_7ON)_4 \cdot 0.5H_2O$				
Green	45.33	2.92	8.23	16.52
	(48.98)	(3.01)	(9.02)	(17.76)
$MoO_2(C_9H_6ON)_2$				
Reddish yellow	52.84	3.17	7.44	23.04
	(51.92)	(2.89)	(6.73)	(23.08)
$WO_2(C_9H_6ON)_2$				
Red	42.91	2.96	5.78	36.86
	(42.86)	(2.38)	(5.56)	(36.51)

[a] Percentages in parentheses are calculated values.

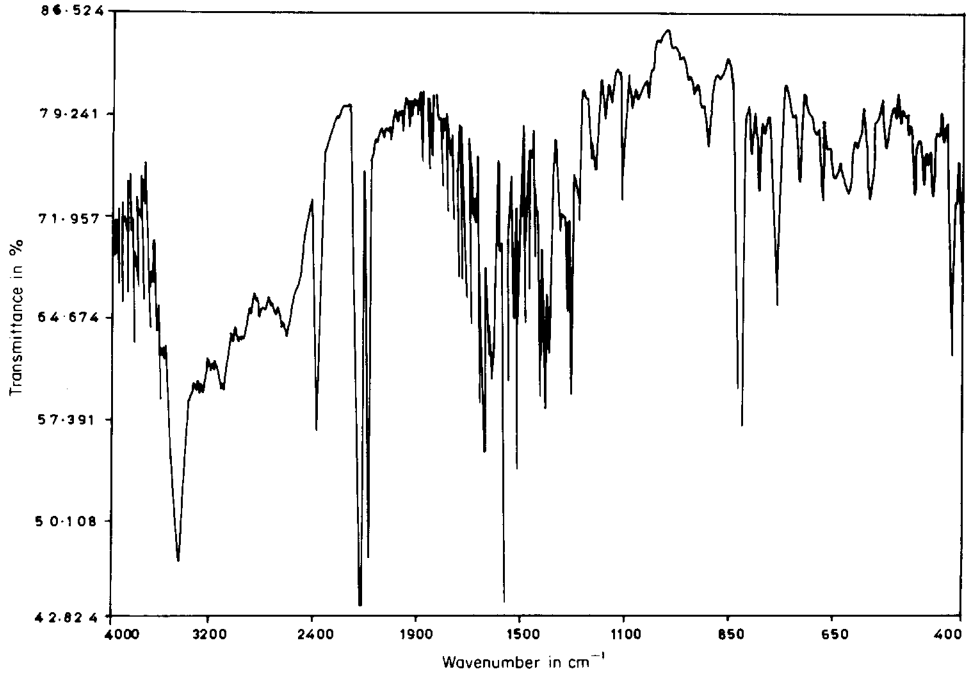

Fig. 1. FTIR spectrum of $K_3[Mo(CN)_7] \cdot (C_9H_7ON)_7 \cdot 5H_2O$.

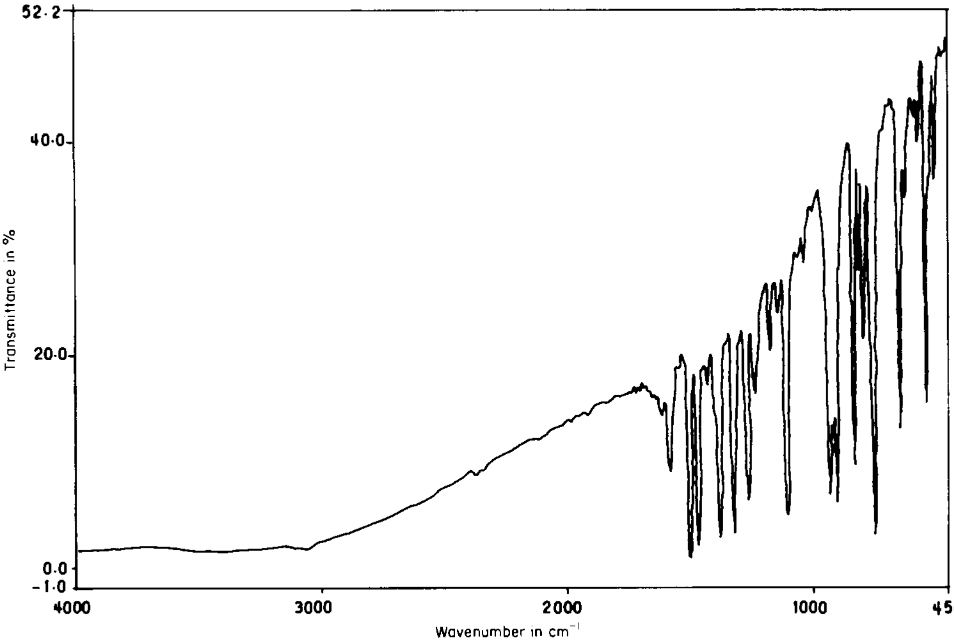

Fig. 2. FTIR spectrum of $MoO_2(C_9H_6ON)_2$.

region 2200–2000 cm^{-1} due to –C≡N stretching. The ν(CN) of free $(CN)^-$ is at 2080 cm^{-1} and in adduct complexes **I** and **II**, the ν(CN) is at 2130 and 2170 cm^{-1} (vs) with a shoulder at 2200 cm^{-1}. The complexes **I** and **II** contain the cyano group. The bands at 2380 cm^{-1} (m) and 2608 cm^{-1} (w) may be due to (NH^+). The broad band at 3424 cm^{-1} is attributed to ν(OH) due to uncoordinated water. The bands found in the range 980–826 cm^{-1} are attributed to $\nu(MoO)_2$. The ν(Mo–O) stretching mode is indicated by the band at 710 cm^{-1}.

The presence of oxine in complexes **I** and **II** is confirmed by the strong band at 1109.6 cm^{-1} for ν(C–O). The complexes **III** and **IV** (Fig. 2, **III**) do not exhibit the ν(CN) band in the range 2200–2000 cm^{-1}. Therefore, the cyanide groups have been replaced by oxine groups. The presence of oxine is confirmed by the bands at 1092.4 and 1123.1 cm^{-1} (s) in complexes **III** and **IV**, the C–O stretching mode. The band observed in the region of 1470–1450 cm^{-1} in the FTIR spectra is attributed to ν(C=N). C=N bands are located at 1509.6 (m), 1470 (s), 1462 (s) and 1486 cm^{-1} (s). The broad band at 748 cm^{-1} (s) in complex **III** is attributed to Mo–O stretching because it is consistent with the metal–oxygen stretch reported for $K_2[OsO_2(CN)_4]$ [14]. Lippard et al. [15] assigned the broad band at 800 cm^{-1} to the Mo–O stretch. In the present investigation, the band observed in the range 858–819 cm^{-1} is attributed to the Mo–O stretch. The ν(N–O) band in complexes **III** and **IV** appears at 1095 (s) and 1092 cm^{-1} (s) respectively.

The presence of two bands in the 930–910 cm^{-1} region (δ_{sym} O=Mo–O$_c$) and the 900–880 cm^{-1} region (δ_{asym} O=Mo=O) in the these compounds is indicative of a cis-dioxo structure [16]. This shift is the result of an increase in the election density on the molybdenum atom which leads to an increase in the repulsive forces with the non-bonding electrons of the atoms of the MoO_2 moiety; hence, a weakening of the Mo–O bond occurs [17].

The FTIR spectra of complexes **I** and **II** exhibit a ν(OH) band at 3500 cm^{-1} (s) due to uncoordinated water. The complexes also exhibit peaks at 1670 cm^{-1} (vs) for ν(C=O) and at 1450 cm^{-1} (s) for ν_{sym} (C–O + C–C).

THERMAL STUDIES

The thermoanalytical data are presented in Table 2.

$[K_3Mo(CN)_7] \cdot (C_9H_7ON)_7 \cdot 5H_2O$

The decomposition of adduct **I**, $[K_3Mo(CN)_7] \cdot (C_9H_7ON)_7 \cdot 5H_2O$, takes place in many steps (Fig. 3). The five molecules of water were evolved at an

TABLE 2

Thermoanalytical data for the decomposition of adduct and complexes

Temp. range in °C	Maximum temp. in DTG in °C	Weight loss in %		Remarks
		Calc.	Obs.	
$K_3[Mo(CN)_7] \cdot (C_9H_7ON)_7 \cdot 5H_2O$				
89.7–150	105.3	5.37	5.51	5 mol of water driven off
165–210	191.8	48.66	47.82	4 mol of oxine removed
211–510	362.3	12.12	11.36	7 cyano moieties removed
511–804	704.9	27.73	27.25	2 mol of oxine decomposed
$K_2WO_2(CN)_2 \cdot (C_9H_7ON)_4 \cdot 0.5H_2O$				
79.7–102	87.7	0.97	1.01	0.5 mol of water removed
101–209	202.6	9.28	8.71	0.6 mol of oxine removed
209–445	426	37.12	35.89	2.4 mol of oxine removed
450–535.5	524.3	15.57	14.06	1 mol of oxine removed
550–810	720	5.59	5.21	2-cyano moieties removed
$MoO_2(C_9H_6ON)_2$				
90–180.5	150.9	8.65	8.30	0.25 mol of oxine decomposed
205–410.2	391.1	34.62	32.34	1 mol of oxine decomposed
420–750	670	25.96	25.89	0.75 mol of oxine removed
$WO_2(C_9H_6ON)_2$				
170–455	432.1	37.14	37.75	1.30 mol of oxine decomposed and removed
465–545.4	539.6	20.0	21.70	0.70 mol of oxine removed

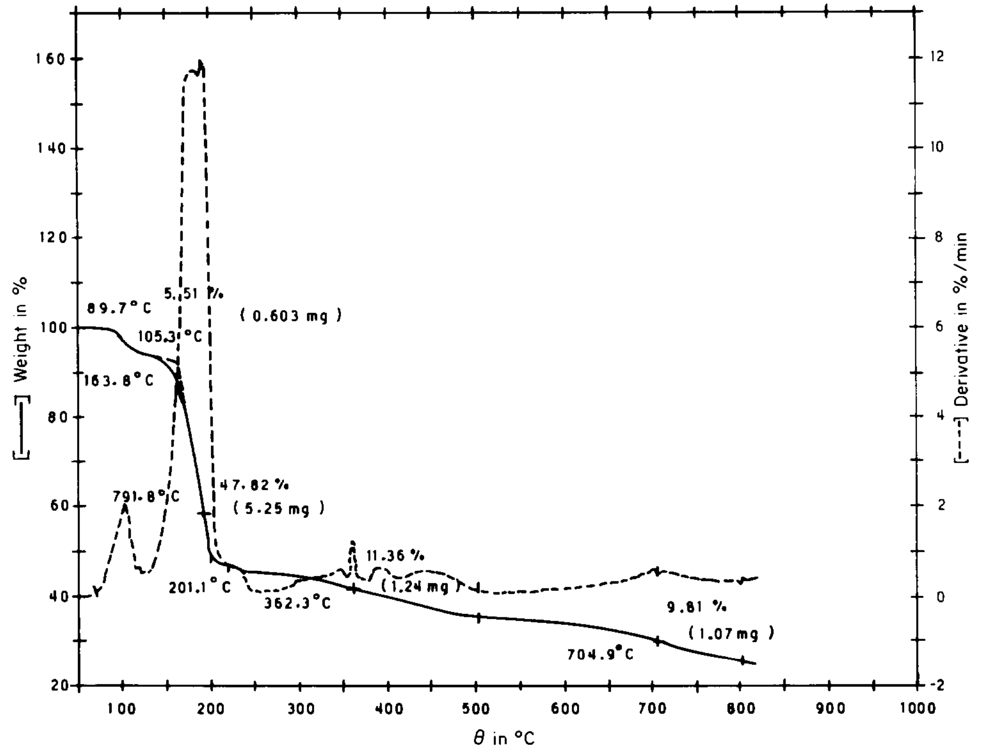

Fig. 3. TGA and DTG curves of $K_3[Mo(CN)_7] \cdot (C_9H_7ON)_7 \cdot 5H_2O$.

onset temperature of 89.7°C, and continued upto 150°C with a DTG maximum at 105 3°C. The observed weight loss is 5.51%, compared with the calculated value of 5.37%. Five molecules of oxine were split off and decomposed at an onset temperature 165°C, and continued upto 210°C with a DTG maximum at 191.8°C. The weight loss is 47.82%, compared with the calculated value of 48.66%. This decomposition step is very steep, displaying the maximum weight loss. In the third step, seven cyanide molecules were removed with an observed weight loss of 11.36% (calculated value of 12.12%). In the next step, two molecules of oxine were decomposed to give the polymeric oxide Mo_3O_8 with the weight remaining being 27.25%, compared with the calculated value of 27.33% [18].

$$K_3[Mo(CN)_7] \cdot (C_9H_7ON)_7 \cdot 5H_2O \xrightarrow[\substack{5.51\% \\ (5.37\%)}]{-5H_2O}$$

$$K_3[Mo(CN)_7] \cdot (C_9H_7ON)_7 \xrightarrow[\substack{47.82\% \\ (48.66\%)}]{-5(C_9H_7ON)} K_3[Mo(CN)_7]$$

$$\cdot\, (C_9H_7ON)_2 \xrightarrow[\substack{11.36\% \\ (12.12\%)}]{-7(CN)} K_3Mo[(C_9H_7ON)_2] \xrightarrow[+O_2]{-2(C_9H_7ON)} \underset{\substack{27.25\% \\ (27.73\%)}}{Mo_3O_8}$$

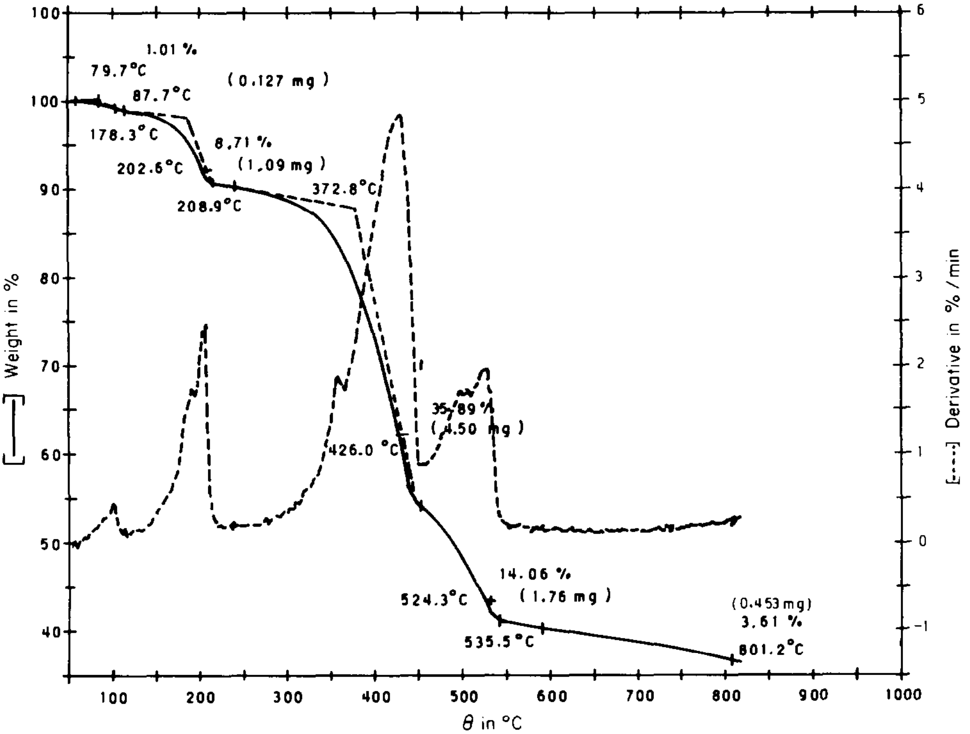

Fig. 4. TGA and DTG curves of $K_3[WO_2(CN)_2] \cdot (C_9H_7ON)_7 \cdot 0.5H_2O$.

$K_2WO_2(CN)_2 \cdot (C_9H_7ON)_4 \cdot 0.5H_2O$

The thermal curves (Fig. 4) of complex **II**, $K_2WO_2(CN)_2 \cdot (C_9H_7ON)_4 \cdot 0.5H_2O$, first indicated the removal of half a molecule of water with an observed weight loss of 1.01% (calculated value of 0.97%), in the range 79.7–102°C with a DTG maximum at 87.7°C. In the second step, 0.6 molecules of oxine was evolved with an observed weight loss of 8.71% (calculated value 9.28%) in the range 101–209°C, with an onset temperature of 178.3°C and the DTG maximum at 202.6°C. In the third step, 2.4 molecules of oxine were decomposed with an observed weight loss of 35.89% (calculated value 37.12%) in the range 209–445°C with an onset temperature of 372.8°C and the DTG maximum at 426°C. In the next step, one molecule of oxine was decomposed with an observed weight loss of 14.06% in the range 450–535.5°C and the DTG maximum at 524.3°C. Finally two cyano groups were decomposed for an observed weight loss of 5.21% (calculated value 5.59%) in the range 550–810°C. A 34.89% weight loss was observed for polymeric oxide (calculated value 35.12%).

$$K_2WO_2(CN)_2 \cdot (C_9H_7ON)_4 \cdot 0.5H_2O \xrightarrow[\substack{1.01\% \\ (0.97\%)}]{-0.5H_2O}$$

$$K_2WO_2(CN)_2 \cdot (C_9H_7ON)_4 \xrightarrow[\substack{8.71\% \\ (9.28\%)}]{-0.6(C_9H_7ON)}$$

$$K_2WO(CN)_2 \cdot (C_9H_7ON)_{3.4} \xrightarrow[\substack{35.89\% \\ (37.12\%)}]{-2.4(C_9H_7ON)}$$

$$K_2WO_2(CN)_2(C_9H_7ON) \xrightarrow[\substack{14.06\% \\ (15.57\%)}]{-(C_9H_7ON)}$$

$$K_2WO_2(CN)_2 \xrightarrow[\substack{5.21\% \\ (5.59\%)}]{-2(CN)+O_2} \underset{\substack{34.89\% \\ (35.12\%)}}{K_2OWO_3}$$

$MoO_2(C_9H_6ON)_2$

The complex $MoO_2(C_9H_6ON)_2$ decomposed with the removal of 0.25 molecule of oxine for the observed weight loss of 8.30%, compared with the calculated value of 8.65%, in the range 90–180.5°C with an onset temperature at 122.6°C and DTG maximum at 150.9°C (Fig. 5). In the second step, one molecule of oxine was evolved with a weight loss of 32.34%, (calculated value of 34.62%) in the range 205–410.2°C with the

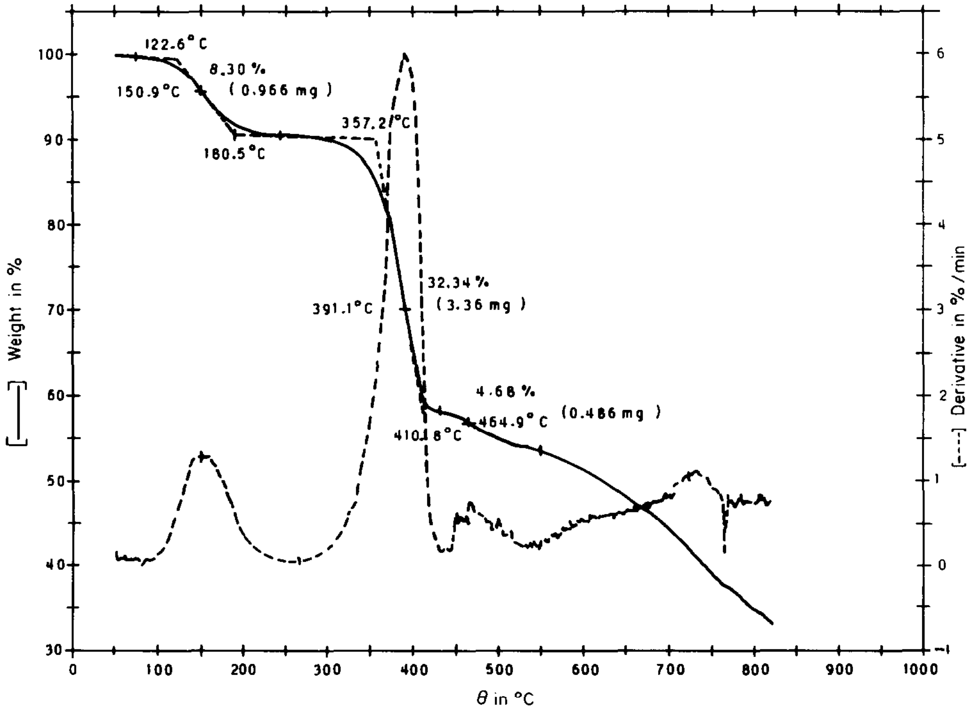

Fig. 5. TGA and DTG curves of $MoO_2(C_9H_6ON)_2$.

DTG maximum at 391.1°C. The difference in the observed and calculated weight losses may be due to overlapping decomposition stages. In the third step, 0.75 molecule of oxine was decomposed and removed in the range 420–750°C for a weight loss of 25.89% (calculated value of 25.96%). Finally, the decomposition product MoO_3 was obtained (33.89%, compared with the calculated value of 34.29%).

$$MoO_2(C_9H_6ON)_2 \xrightarrow[\substack{8.30\% \\ (8.65\%)}]{-0.25(C_9H_6ON)}$$

$$MoO_2(C_9H_6ON)_{1.75} \xrightarrow[\substack{32.34\% \\ (34.62)}]{-(C_9H_6ON)}$$

$$MoO_2(C_9H_6ON)_{0.75} \xrightarrow[\substack{25.89\% \\ (25.96\%)}]{-0.75(C_9H_6ON)} \underset{\substack{33.89\% \\ (34.29\%)}}{MoO_3}$$

$WO_2(C_6H_6ON)_2$

The complex $WO_2(C_9H_6ON)_2$ first fragmented losing 1.30 molecules of oxine with an observed weight loss of 37.75%, compared with the calculated value of 37.14%, in the range 170–455°C with an onset temperature of 380.1°C and a DTG maximum at 431.2°C (Fig. 6). The

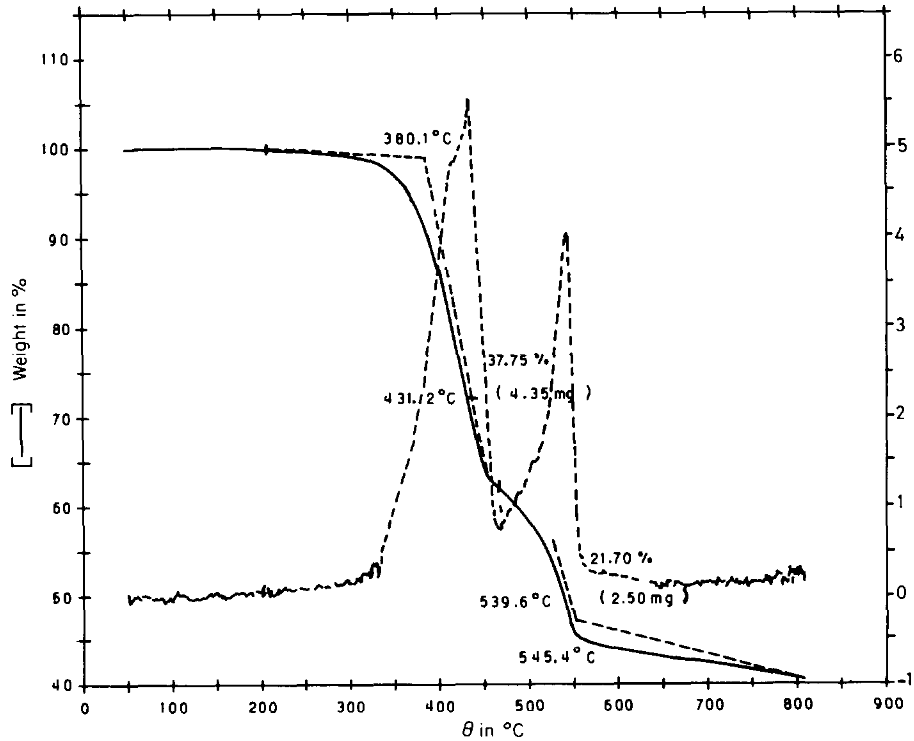

Fig. 6. TGA and DTG curves of $WO_2(C_9H_6ON)_2$.

second decomposition step was the loss of 0.70 molecules of oxine in the range 465–545.4°C with a DTG maximum at 539.6°C for an observed weight loss of 21.70%, compared with the calculated value of 20.0%. The end product was WO_3 with an observed weight loss of 46.0% (calculated value 46.10%),

$$WO_2(C_6H_6ON)_2 \xrightarrow[\substack{37.75\% \\ (37.14\%)}]{-1.3(C_9H_6ON)} WO_2(C_9H_6ON)_{0.7} \xrightarrow[\substack{21.70\% \\ (20.0\%)}]{-0.7(C_9H_6ON)} \underset{\substack{46.03\% \\ (46.10\%)}}{WO_3}$$

Computation of the kinetic parameters

The thermograms indicate that the decomposition of complexes **I–III** display a very steep second step while, in complex **IV**, the first decomposition step is very steep. The conversion occurs over a relatively small temperature range. The activation energy E_a may be calculated from the equation

$$\log\frac{\rho_T}{W}=\frac{E_a}{4.6T}+\log\frac{Z}{(RH)}$$

where $\rho_T = -dw/dt$ and (RH) is the heating rate.

The graphs of $\log[-\ln(1-\alpha)/T^2]$ versus $1/T \times 10^3$ and $-\log k$ versus $1/T \times 10^3$ were plotted for the complexes **I–IV** (see Fig. 7 for **I**). A straight line was obtained for the decomposition stage. The activation energy E_a

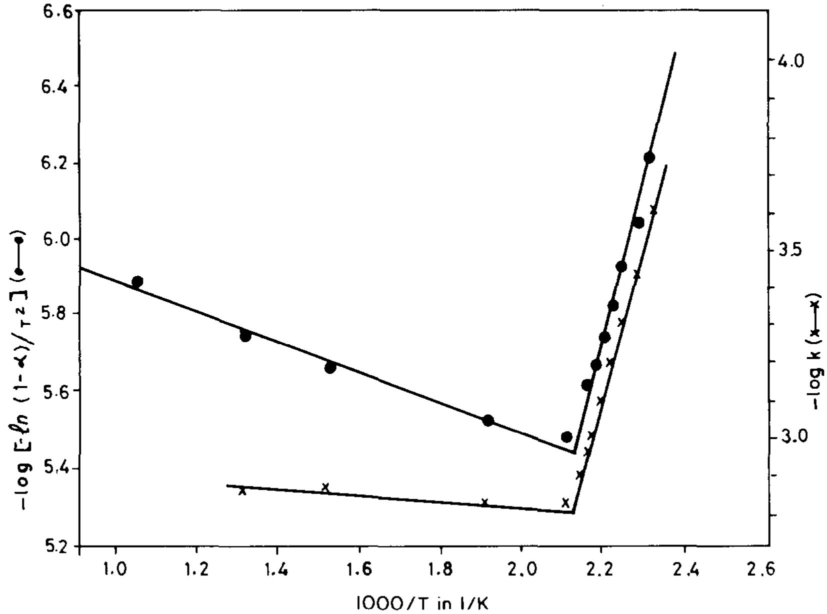

Fig. 7. $-\log[-\ln(1-\alpha)/T^2]$ vs. $1/T \times 10^3$ and $\log k$ vs. $1/T \times 10^3$ for $K_3[Mo(CN)_7] \cdot (C_9H_7ON)_7 \cdot 5H_2O$.

was calculated from the slope of the curve using the equation

$E_a = -4.6 \times \text{slope}$

The activation energy of $K_3[Mo(CN)_7] \cdot (C_9H_7ON) \cdot 5H_2O$ (**I**) was found to be 18.6 kcal mol^{-1} for the conversion from 5%–40% while the activation energy of $K_2WO_2(CN)_2 \cdot (C_9H_7ON)_4 \cdot 0.5H_2O$ (**II**) was found to be 11.5 kcal mol^{-1} for the conversion from 10%–45%. The activation energies for the second decomposition of complex **III** step and for the first decomposition step of complex **IV** were calculated as 18.4 kcal mol^{-1} for conversion from 10%–40% and 23 kcal mol^{-1} for conversion from 10%–40%, respectively.

The activation energy was also determined from the Arrhenius equation by plotting $\log k$ versus $1/T \times 10^3$ for all the complexes (see Fig. 8 for **IV**). The TG data were analysed using the Coats and Redfern treatment [19]. The values of $\log[-\ln(1-\alpha)/T^2]$ versus $1/T \times 10^3$ were plotted (Fig. 8, **IV**) and straight lines were obtained for the individual decomposition steps, indicating that the order of reaction for decomposition of all the complexes is one. The activation energies of complexes **I**, **II**, **III** and **IV** were found to be 19.25, 12.9, 18.09 and 21.07 kcal mol^{-1}, respectively, which are fairly close to the activation energies calculated by the other methods.

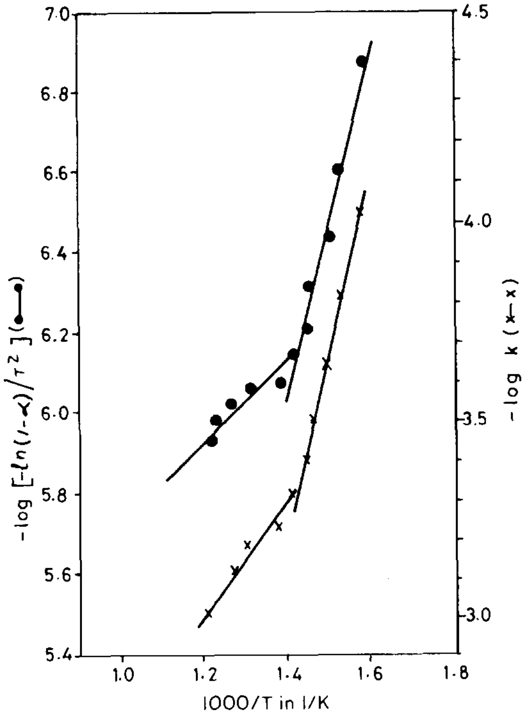

Fig. 8. $-\text{Log}[-\ln(1-\alpha)/T^2]$ vs. $1/T \times 10^3$ and $\log k$ vs. $1/T \times 10^3$ for $WO_2(C_9H_6ON)_2$.

The TG and DTG thermograms show that the complex $WO_2(C_9H_6ON)_2$ (**IV**) is the most stable.

ACKNOWLEDGEMENT

One of the authors (N.K.S.P.) is grateful to Professor D.V. Singh, Director, Central Road Research Institute, New Delhi, for permission to work in JMI.

REFERENCES

1 V. Balzani and V. Carassiti, Photo-Chemistry of Cordination Compounds, Academic Press, London, New York, 1970.
2 Z. Strasicka and H. Bulska, Rocz. Chem., 47 (1973) 1365.
3 D. Kiessling, E. Nagorsnik, P. Thomas and H. Hennig, J. Prakt. Chem., 322 (1980) 843.
4 H. Hennig, E. Koyer, E. Lippmann, E. Nagorsnik, P. Thomas and M. Weissengels, J. Signalaufzeichnungs-materialien, 6 (1978) 39.
5 H. Hennig, P. Thomas, R. Wagener, D. Rehorck and K. Jurdeczka, Z. Chem., 17 (1977) 241.
6 P. Thomas, C. Saidi and H. Hennig, Z. Chem., 18 (1978) 148.
7 P. Thomas, C. Saidi and H. Hennig, Inorg. Chim. Acta, 82 (1984) L11–12.
8 S.I. Ali and Harpal Kaur, Bull. Chem. Soc. Jpn., 63 (1990) 3615.
9 S.I. Ali and Harpal Kaur, Transition Met. Chem., 16 (1991) 450.
10 S.I. Ali and N.K.S. Pundhir, Thermochim. Acta, 189 (1991) 97.
11 S.I. Ali and N.K.S. Pundhir, J. Therm. Anal., 38 (1992) 1391.
12 J.G. Leipoldt, L.D.C. Bok and P.T.Z. Collier, Z. Anorg. Allg. Chem., 407 (1974) 350; 409 (1974) 343.
13 A.I. Vogel, A Text Book of Quantitative Inorganic Analysis, Longman, London, 1982.
14 W.P. Griffith, J. Chem. Soc., 45 (1964) 245.
15 S.J. Lippard, H. Nizaki and B.J. Russ, Chem. Commun., 3 (1967) 119.
16 A. Syamal and D. Kumar, Transition Met. Chem., 7 (1982) 118.
17 J. Goffart, J.P. Mevnier and G. Duyckaerto, Inorg. Nucl. Chem. Lett., 14 (1980) 233.
18 P. Caillet and P. Saumagne, J. Mol. Struct., 4 (1969) 351.
19 A.W. Coats and J.P. Redfern, J. Polym. Sci. Part B, 3 (1965) 1917.